STOCHASTIC DECOMPOSITION AND APPLICATION TO PROBABILISTIC DYNAMICS

By Yousun Li[1] and Ahsan Kareem,[2] Member, ASCE

ABSTRACT: The frequency-domain analysis concerning the response of nested-cascade multiple input/output systems requires computation of the cross-spectral density matrices that involve the input, intermediate, and output vectors. Clearly, as the number of nested systems increases, the order of the cross-spectral density matrix increases, demanding additional computational effort. This feature lessens the computational attractiveness of the frequency-domain analysis. A stochastic decomposition technique is developed that improves the efficiency of conventional frequency-domain analysis by eliminating the intermediate step of estimating cross-spectral density matrices. Central to this technique is the decomposition of a set of correlated random processes into a number of component random processes. Statistically, any two processes decomposed in this manner are either fully coherent or noncoherent. A random subprocess obtained from this decomposition is expressed in terms of a decomposed spectrum. A theoretical basis for this approach and computational procedures for carrying out such decompositions in probabilistic dynamics are presented.

INTRODUCTION

The frequency-domain analysis is frequently used in the response analysis of linear dynamic systems subjected to stochastic loads primarily for its computational efficiency and concise and clear relationship among various load and response processes. A multivariate process is characterized in the frequency domain by its cross-spectral density matrix. The cross-spectral density matrices of the input and output of a linear dynamic system are related by a transfer function matrix. However, if the dynamic system consists of a number of nested-cascade systems (Fig. 1), a significant amount of central processing unit (CPU) time is needed for the computation of the cross-spectral density functions involving the initial input, and the intermediate and final outputs. This feature lessens the computational attractiveness of the frequency-domain approach.

Typical examples for such systems may be found in the perturbation and iteration solution techniques that are often used for the analysis of nonlinear dynamic systems following a linearization or a quadratization of the nonlinearity. In a perturbation technique, the equations at different perturbation orders can be regarded as nested-cascade systems, in which the cross-spectral density functions between the responses at different orders are required for the final solution. Similarly, in an iteration procedure, the cross-spectral density functions between the input and the output obtained in the previous iteration are computed to account for the feedback. Therefore, computation of the cross-spectral density functions in both perturbation and iteration procedures for systems with large degrees of freedom, and multicorrelated input/output, may become an arduous task. For example, the analysis of offshore platforms exposed to random loads poses difficulty due to nonlinear dependence of wave-induced loads on the wave-particle kinematics and the structural response. The equation of motion can be solved by a perturbation or by an iteration procedure after an equivalent statistical linearization or quadratization. The application of these solution techniques to jacket-type platforms may be found in Deleuil et al. (1986), Eatock-Taylor and Rajagopalan (1982), Lipsett (1986), and Grecco and Hudspeth (1983). However, for moored floating structures, (e.g., tension leg platforms), the problem is more complex due to the dynamic nonlinearity in the applied loading that precludes straightforward application of iteration and perturbation techniques.

In view of this shortcoming, a technique, referred to as stochastic decomposition, has been developed in the present study. This technique decomposes a set of random processes into component random processes, the relationship between any two of which is either fully coherent or noncoherent. Each component process is described by a corresponding decomposed spectrum, which is related to conventional spectral description, for example, a spectral density function. Any linear transformation that relates a set of random processes also relates the corresponding decomposed spectral description of these processes. The fully coherent or noncoherent relationship between the decomposed processes alleviates the need for the computation of the cross-

[1]Res. Engr., Shell Development Co., Houston, TX 77001-0481.
[2]Prof., Dept. of Civ. Engrg. & Geological Sci., Univ. of Notre Dame, Notre Dame, IN 46556-0767.

Note. Discussion open until June 1, 1995. To extend the closing date one month, a written request must be filed with the ASCE Manager of Journals. The manuscript for this paper was submitted for review and possible publication on March 10, 1993. This paper is part of the ***Journal of Engineering Mechanics***, Vol. 121, No. 1, January, 1995. ©ASCE, ISSN 0733-9399/95/0001-0162–0174/$2.00 + $.25 per page. Paper No. 27053.

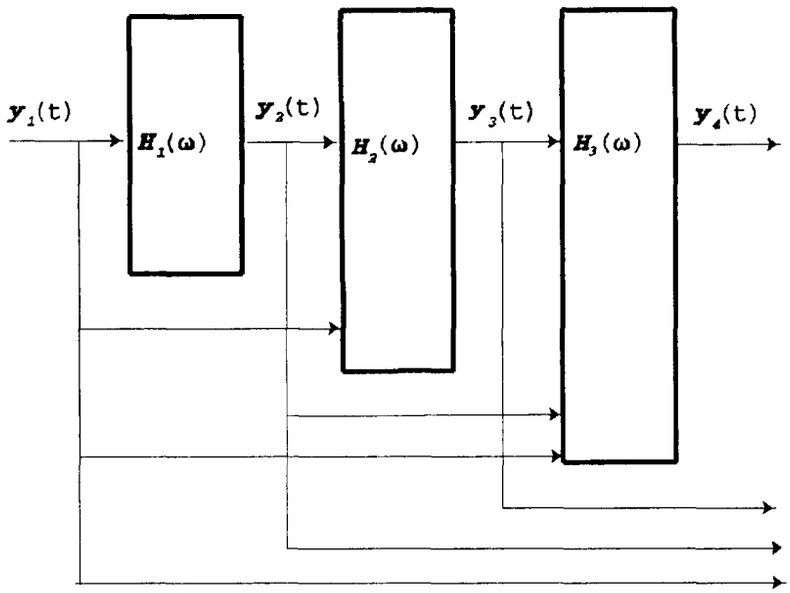

FIG. 1. Nested-Cascade System

spectral density function, thus enhancing the computational efficiency of the frequency-domain approach.

The examples of the concept can be found in probabilistic mechanics. For example, the simulation of random processes, in which each random process is the sum of noncoherent component processes generated by Fourier transformation [e.g., Shinozuka (1963)]. Bendat (1976) and Dodds and Robson (1975) decomposed input processes into noncoherent processes for optimal linear operations for engine-noise detection. In the present study, emphasis is placed on the application of such a decomposition in the frequency-domain analysis of a nested-cascade dynamic system. The decomposition concept was extended to the quadratic dynamic systems that will be addressed in a forthcoming report.

SPECTRAL DESCRIPTION OF NESTED-CASCADE SYSTEMS

A nested-cascade system consists of a number of linear subsystems closed in series, in which the output of a subsystem becomes part of the input to the following subsystems. For each subsystem, from the given spectral descriptions of the input time processes, the output spectral density functions and the statistical relationship between input and output can be calculated through transfer functions. The computation of the system output from the input involves evaluation of the intermediate processes that links different subsystems. Hence, not only are the spectral density functions of the output of each subsystem needed, but the relationship among all the processes, including input, intermediate, and the required system output, needs to be computed in terms of the cross-spectral density functions. To explain this further, it is necessary to examine a typical nested-cascade system shown in Fig. 1. The subsystem 1 is excited by a correlated input vector $\mathbf{y}_1(t)$ containing N_1 processes. The output of subsystem 1 is described by the vector $\mathbf{y}_2(t)$ consisting of N_2 processes, and subsystem 2 is excited by $\mathbf{y}_1(t)$ and $\mathbf{y}_2(t)$, and so on. The power spectral density functions of the output of each subsystem are obtained by the following equations:

$$\mathbf{G}_2(\omega) = \mathbf{H}_1(\omega)\mathbf{G}_1(\omega)\mathbf{H}_1^*(\omega); \qquad \mathbf{G}_{21}(\omega) = \mathbf{H}_1(\omega)\mathbf{G}_1(\omega) \tag{1a,b}$$

$$\mathbf{G}_3(\omega) = \mathbf{H}_2(\omega)\begin{bmatrix}\mathbf{G}_1(\omega) & \mathbf{G}_{12}^*(\omega)\\ \mathbf{G}_{12}(\omega) & \mathbf{G}_2(\omega)\end{bmatrix}\mathbf{H}_2^*(\omega); \qquad \begin{bmatrix}\mathbf{G}_{31}(\omega)\\ \mathbf{G}_{32}(\omega)\end{bmatrix} = \mathbf{H}_2(\omega)\begin{bmatrix}\mathbf{G}_1(\omega) & \mathbf{G}_{12}^*(\omega)\\ \mathbf{G}_{12}(\omega) & \mathbf{G}_2(\omega)\end{bmatrix} \tag{1c,d}$$

$$\mathbf{G}_4(\omega) = \mathbf{H}_3(\omega)\begin{bmatrix}\mathbf{G}_1(\omega) & \mathbf{G}_{12}^*(\omega) & \mathbf{G}_{13}^*(\omega)\\ \mathbf{G}_{12}(\omega) & \mathbf{G}_2(\omega) & \mathbf{G}_{23}^*(\omega)\\ \mathbf{G}_{13}(\omega) & \mathbf{G}_{23}(\omega) & \mathbf{G}_3(\omega)\end{bmatrix}\mathbf{H}_3^*(\omega) \tag{1e}$$

where $\mathbf{G}_i(\omega)$ = the spectral density matrix function of $\mathbf{y}_i(t)$; $\mathbf{G}_{ij}(\omega)$ = the cross-spectral density matrix between processes $\mathbf{y}_i(t)$ and $\mathbf{y}_j(t)$; $\mathbf{H}_i(\omega)$ denotes the transfer function matrix of the ith subsystem; and $*$ is the transpose and conjugate operator. With an increase in the number of nested-cascade systems, the size of the spectral matrix increases concomitantly. Examples of a cascade system can be found in the procedures used in the solution of nonlinear dynamic systems. Let $\mathbf{x}(t)$ be a set of time series of responses under an exciting load vector $\mathbf{f}(t)$. For a weakly

nonlinear system, perturbation techniques may be used for the spectral analysis of this system, for example, Lipsett (1986) and Eatock-Taylor and Rajagopalan (1982) used perturbation for the response spectral density functions of fixed offshore platforms. This method is based on the assumption that

$$\mathbf{x}(t) = \sum_{r=0}^{\infty} \varepsilon^{[r]} \mathbf{x}^{r}(t) \tag{2}$$

in which the perturbation parameter $\varepsilon << 1$; and the superscript $[r]$ is the perturbation order. For $r = 0$

$$\mathbf{x}^{[0]}(t) = L^{[0]}(\mathbf{f}(t)) \tag{3a}$$

where $L^{[0]} =$ a linear operator. For $r \neq 0$

$$\mathbf{x}^{[r]}(t) = L^{[r]}(\mathbf{x}^{[0]}(t), \mathbf{x}^{[1]}(t), \ldots, \mathbf{x}^{[r-1]}(t)) \tag{3b}$$

where the linear operator, $L^{[r]}$ is formed according to the response obtained in the previous perturbations. The transfer function $\mathbf{H}^{[r]}(\omega)$, a function of the statistics of $\Sigma_{s=0}^{r-1} x^{[s]}(t)$, corresponds to $L^{[r]}$. Fig. 2(a) illustrates the perturbation procedure represented by a nested-cascade system. The spectral transformation in each subsystem is given as follows:

$$\mathbf{G}_{x^{[0]}}(\omega) = \mathbf{H}^{[0]}(\omega)\mathbf{G}_{f}(\omega)\mathbf{H}^{[0]*}(\omega); \qquad \mathbf{G}_{x^{[1]}}(\omega) = \mathbf{H}^{[1]}(\omega)\mathbf{G}_{x^{[0]}}(\omega)\mathbf{H}^{[1]*}(\omega) \tag{4a,b}$$

$$\mathbf{G}_{x^{[2]}}(\omega) = \mathbf{H}^{[2]}(\omega) \begin{Bmatrix} \mathbf{G}_{x^{[0]}}(\omega) & \mathbf{G}_{x^{[1]}x^{[0]}}(\omega) \\ \mathbf{G}_{x^{[0]}x^{[1]}}(\omega) & \mathbf{G}_{x^{[1]}}(\omega) \end{Bmatrix} \mathbf{H}^{[2]*}(\omega) \tag{4c}$$

If the dimension of $\mathbf{x}(t)$ is N, then the dimensions of $\mathbf{H}^{[2]}(\omega)$ are $(N, 2N)$. The cross-spectral density matrix of the response is given by

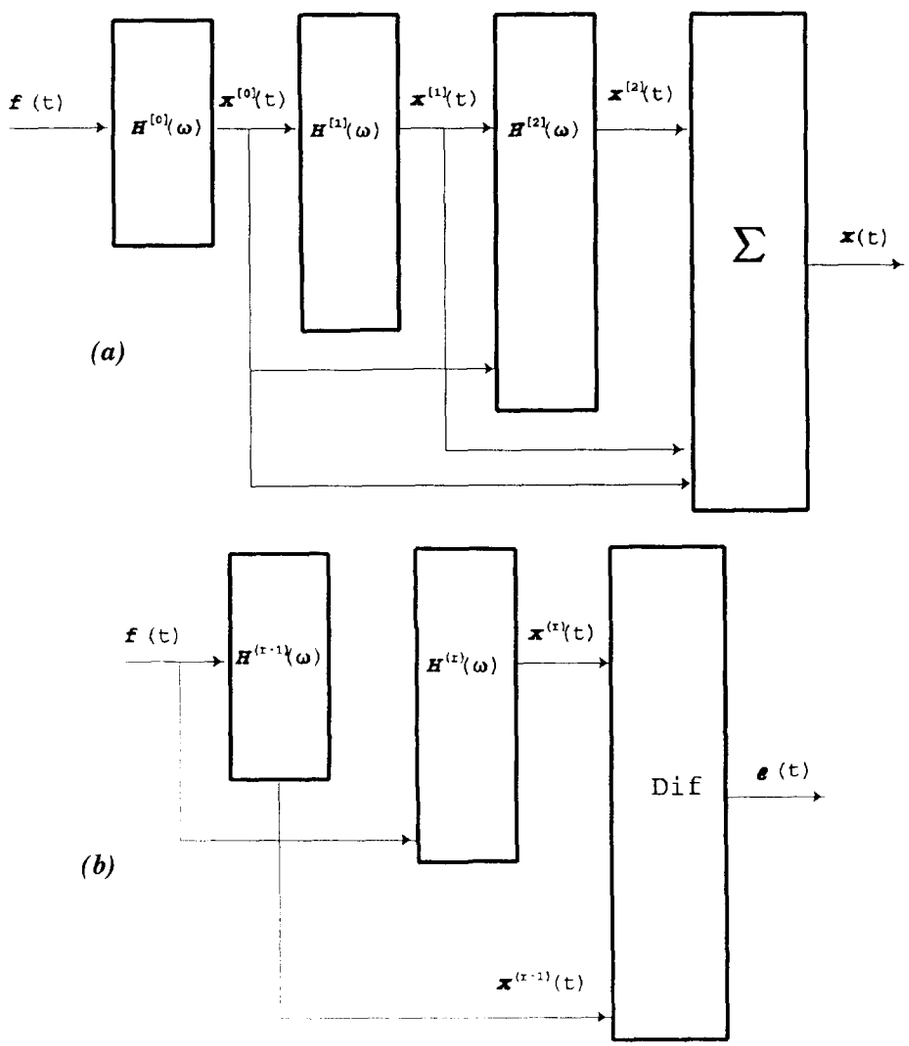

FIG. 2. Schematic Representation: (a) Perturbation Procedure; and (b) Iteration Procedure

$$\mathbf{G}_y(\omega) = \sum_{r=0}^{\infty} \sum_{s=0}^{\infty} \mathbf{G}_{x^{[r]}x^{[s]}}(\omega) \tag{5}$$

which involves significant computational effort to evaluate the correlations among responses at various perturbation orders. Considering up to third-order terms for illustrative purposes, the previous equation is given by

$$\mathbf{G}_y(\omega) \overset{\text{Re}}{\approx} \mathbf{G}_{x^{[0]}}(\omega) + 2\varepsilon\mathbf{G}_{x^{[0]}x^{[1]}}(\omega) + \varepsilon^2\mathbf{G}_{x^{[1]}}(\omega) + 2\varepsilon^2\mathbf{G}_{x^{[0]}x^{[2]}}(\omega) + 2\varepsilon^3\mathbf{G}_{x^{[0]}x^{[3]}}(\omega) + 2\varepsilon^3\mathbf{G}_{x^{[1]}x^{[2]}}(\omega) \tag{6}$$

The cross-spectral density functions in the preceding equations are computed by

$$\mathbf{G}_{x^{[0]}x^{[1]}}(\omega) = \mathbf{G}_{x^{[0]}}(\omega)\mathbf{H}^{[1]*}(\omega) \tag{7a}$$

and

$$\begin{bmatrix} \mathbf{G}_{x^{[0]}x^{[2]}}(\omega) \\ \mathbf{G}_{x^{[1]}x^{[2]}}(\omega) \end{bmatrix} = \begin{bmatrix} \mathbf{G}_{x^{[0]}}(\omega) & \mathbf{G}_{x^{[1]}x^{[0]}}(\omega) \\ \mathbf{G}_{x^{[0]}x^{[1]}}(\omega) & \mathbf{G}_{x^{[2]}}(\omega) \end{bmatrix} \mathbf{H}^{[2]*}(\omega) \tag{7b}$$

With an increase in the perturbation order, more cross-spectral density functions must be computed.

The second approach for the solution of the nonlinear dynamic equation is the iteration technique. Let us assume that the nonlinear equations can be linearized as

$$\mathbf{x}(t) = L^{\sigma}(\mathbf{f}(t)) \tag{8}$$

where the linear operator L^{σ} denotes the dependency of the linear transform on the statistics of the response parameters (e.g., variance). Athe the rth iteration, the transformation is carried out by

$$\mathbf{G}_{x^{(r)}}(\omega) = \mathbf{H}^{(r)}(\omega)\mathbf{G}_f(\omega)\mathbf{H}^{(r)*}(\omega) \tag{9}$$

in which $\mathbf{H}^{(r)}(\omega)$ is evaluated based on the response spectra, $\mathbf{G}_{x^{(r-1)}}(\omega)$, computed at the previous iteration. An example in using the iteration technique in the spectral analysis of offshore structures can be found in Grecco and Hudspeth (1983).

For the case in which a robust criterion for iteration convergence is required, let us define an error time series $e(t)$, which can be viewed as a linear transform of the response from the present and previous iterations

$$e(t) = \mathbf{x}^{(r)}(t) - \mathbf{x}^{(r-1)}(t) \tag{10}$$

The spectral and cross-spectral density functions of the error time series are used to determine the convergence

$$\mathbf{G}_e(\omega) = \mathbf{G}_{x^{(r)}}(\omega) + \mathbf{G}_{x^{(r-1)}}(\omega) - 2\,\text{Re}(\mathbf{G}_{x^{(r)}x^{(r-1)}}(\omega)) \tag{11}$$

The cross-spectral density between the two iteration response components is given by

$$\mathbf{G}_{x^{(r)}x^{(r-1)}}(\omega) = \mathbf{H}^{(r)}(\omega)\mathbf{G}_f(\omega)\mathbf{H}^{(r-1)*}(\omega) \tag{12}$$

Fig. 2(b) shows a cascade system representing the iteration procedure. Iteration continues until $\mathbf{G}_e(\omega)$ is within a prescribed limit.

The above two examples demonstrate that, during the spectral analysis, one has to keep track of the relationships among the input, output, and intermediate random processes in terms of the cross-spectral density functions. Sometimes, a cascade system may contain many more subsystems than shown in these examples, or each subsystem may have a large dimension or both. Therefore, the cross-spectral–density-function computation may become further complicated and must require a significant additional CPU time.

DECOMPOSED SPECTRA AND THEIR PHYSICAL INTERPRETATION

The decomposed spectral matrix $\mathbf{D}_y(\omega)$ (dimension as M, Λ), of a set of random processes $\mathbf{y}(t)$, is complex, and is defined as

$$\mathbf{D}_y(\omega)\mathbf{D}_y^*(\omega) = \mathbf{G}_y(\omega) \tag{13}$$

The element in the μth row and λth column in matrix $\mathbf{D}_y(\omega)$ is denoted by $D_{y_{\mu/\lambda}}(\omega)$. A slash is added between the subscripts μ and λ since $D_{y_{\mu/\lambda}}(\omega)$ does not only indicate an element in a matrix, but, it also has a certain physical meaning that is addressed later. Let us define the μth row of $\mathbf{D}_y(\omega)$ in terms of the following decomposed spectral vector:

$$\mathbf{D}_{y_\mu}(\omega) = \begin{Bmatrix} D_{y_{\mu/1}}(\omega) \\ D_{y_{\mu/2}}(\omega) \\ \vdots \\ D_{y_{\mu/j}}(\omega) \\ \vdots \\ D_{y_{\mu/\Lambda}}(\omega) \end{Bmatrix} \tag{14a}$$

Similarly, define each column of the matrix $\mathbf{D}_y(\omega)$ by the following vector:

$$\mathbf{D}_{y_{/\lambda}}(\omega) = \begin{Bmatrix} D_{y_{1/\lambda}}(\omega) \\ D_{y_{2/\lambda}}(\omega) \\ \vdots \\ D_{y_{\mu/\lambda}}(\omega) \\ \vdots \\ D_{y_{M/\lambda}}(\omega) \end{Bmatrix} \tag{14b}$$

The decomposed spectral matrices and the vectors defined above have many useful attributes, which are summarized in the following. The decomposed spectral vector $\mathbf{D}_{y_\mu}(\omega)$ is linearly related to $y_\mu(t)$. For example, if

$$y_\mu(t) = \alpha y_{\mu'}(t) + \beta y_{\mu''}(t) \tag{15a}$$

then

$$\mathbf{D}_{y_\mu}(\omega) = \alpha \mathbf{D}_{y_{\mu'}}(\omega) + \beta \mathbf{D}_{y_{\mu''}}(\omega) \tag{15b}$$

The linear transformation of a set of random processes can be realized by the linear transformation of its decomposed spectral matrix. If $\mathbf{y}(t)$ and $\mathbf{z}(t)$ are linearly related through a transfer function $\mathbf{H}_{yz}(\omega)$, then their decomposed spectral matrices are related by

$$\mathbf{D}_z(\omega) = \mathbf{H}_{zy}(\omega)\mathbf{D}_y(\omega) \tag{16a}$$

where

$$\mathbf{G}_y(\beta) = \mathbf{D}_y(\omega)\mathbf{D}_y^*(\omega) \qquad \text{and } \mathbf{G}_z(\omega) = \mathbf{D}_z(\omega)\mathbf{D}_z^*(\omega) \tag{16b}$$

If two sets of random processes $\mathbf{y}(t)$ and $\mathbf{z}(t)$ are linearly related by $\mathbf{H}_{zy}(\omega)$ as shown in (16), and $\mathbf{w}(t)$ is a random process vector consisting of processes $\mathbf{y}(t)$ and $\mathbf{z}(t)$, then the decomposed spectral matrix of $\mathbf{w}(t)$ is simply a stacked matrix of $\mathbf{D}_y(\omega)$ and $\mathbf{D}_z(\omega)$

$$\mathbf{D}_w(\omega) = \begin{bmatrix} \mathbf{D}_y(\omega) \\ \mathbf{D}_z(\omega) \end{bmatrix} \tag{17}$$

These properties lead to the physical interpretation of the decomposed spectra. This interpretation is referred to here as stochastic decomposition. In this concept, each random process $y_\mu(t)$ is decomposed into a number of component processes $y_{\mu/\lambda}(t)$ such that

$$y_\mu(t) = \sum_{\lambda=1}^{\Lambda} y_{\mu/\lambda}(t) \tag{18}$$

in which, $y_{\mu/\lambda}(t)$ and $y_{\mu'/\lambda'}(t)$ are noncoherent if $\lambda \neq \lambda'$, and fully coherent if $\lambda = \lambda'$. This decomposition is sketched in Fig. 3. The component processes are related to the corresponding decomposed spectra. The spectral density function of $y_{\mu/\lambda}(t)$ is

$$G_{y_{\mu/\lambda}}(\omega) = D_{y_{\mu/\lambda}}(\omega)\overline{D_{y_{\mu/\lambda}}(\omega)} \tag{19a}$$

and the cross-spectral density function is given by

$$G_{y_{\mu/\lambda}y_{\mu'/\lambda}}(\omega) = D_{y_{\mu/\lambda}}(\omega)\overline{D_{y_{\mu'/\lambda}}(\omega)} \tag{19b}$$

where the overbar denotes conjugate. Corresponding to (14*a*) and (14*b*), let us define two vectors for the subprocesses:

$$\mathbf{y}_{\mu/}(t) = \begin{Bmatrix} y_{\mu/1}(t) \\ y_{\mu/2}(t) \\ \vdots \\ y_{\mu/\lambda}(t) \\ \vdots \\ y_{\mu/\Lambda}(t) \end{Bmatrix} \tag{20a}$$

in which all the elements are the components of $\mathbf{y}_\mu(t)$ and mutually noncoherent, and

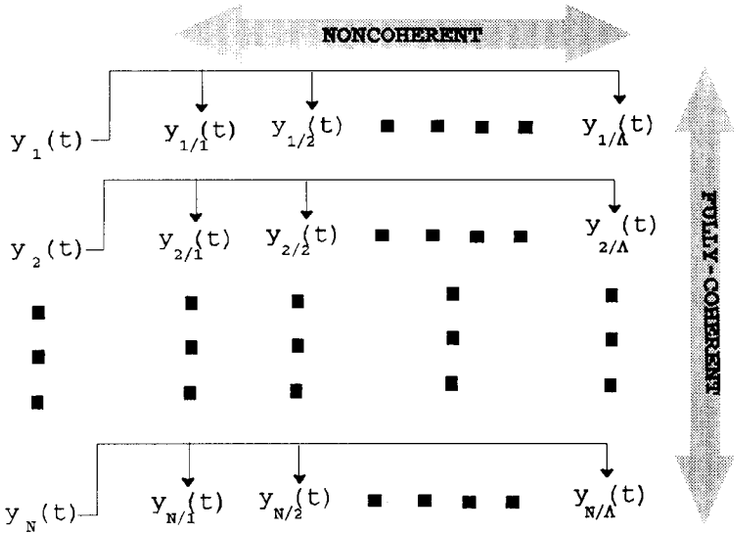

FIG. 3. Schematic Representation of Stochastic Decomposition Scheme

$$\mathbf{y}_{/\lambda}(t) = \begin{Bmatrix} y_{1/\lambda}(t) \\ y_{2/\lambda}(t) \\ \cdot \\ \cdot \\ y_{i/\lambda}(t) \\ \cdot \\ \cdot \\ y_{M/j}(t) \end{Bmatrix} \tag{20b}$$

contains all the component processes that belong to different parent processes, but these are fully coherent. Each component process is described in the frequency domain by the decomposed spectrum that is a complex function. The modulus of the complex function is related to its spectral density function, and its argument is the phase difference with other component processes fully coherent with it.

Since any two component processes are either fully coherent or noncoherent, the computation of the cross-spectral density functions is no longer required. Now we can return to the nested-cascade system described by (1). Following stochastic decomposition concepts, a given spectral matrix $\mathbf{G}_1(\omega)$ is first decomposed into $\mathbf{D}_1(\omega)$, according to (13). Then the following transformations are performed:

$$\mathbf{D}_2(\omega) = \mathbf{H}_1(\omega)\mathbf{D}_1(\omega); \qquad \mathbf{D}_3(\omega) = \mathbf{H}_2(\omega)\begin{bmatrix} \mathbf{D}_1(\omega) \\ \mathbf{D}_2(\omega) \end{bmatrix}; \qquad \mathbf{D}_4(\omega) = \mathbf{H}_3(\omega)\begin{bmatrix} \mathbf{D}_1(\omega) \\ \mathbf{D}_2(\omega) \\ \mathbf{G}_3(\omega) \end{bmatrix} \tag{21a-c}$$

It is noted that with an increase in the number of subsystems, the decomposed spectral matrix experiences only an increase in its row dimension, and the column dimension remains unchanged. In contrast to this formulation, the dimension of matrices increases in the conventional approach [(1)]. As stated earlier, in this scheme the need to compute the cross-spectral density functions is eliminated. If it is required, the spectral density function of any process or the cross-spectral density function between any two processes can be derived from the decomposed spectra by a simple computation.

Let us now rearrange all the input and output processes of the subsystems and use $\mathbf{D}(\omega)$ to denote the decomposed spectral matrix of all the input, intermediate, and output processes. The spectral density function of the μth process is given by

$$G_{\mu}(\omega) = \mathbf{D}^*_{\mu/}(\omega)\mathbf{D}_{\mu/}(\omega) \tag{22a}$$

and the cross-spectral density function between the μth and μ'th processes is

$$G_{\mu\mu'}(\omega) = \mathbf{D}^*_{\mu/}(\omega)\mathbf{D}_{\mu'/}(\omega) \tag{22b}$$

The stochastic decomposition can be used in the perturbation and iteration procedures used in the fequency-domain analysis. As a first step in the application of the stochastic decomposition in the frequency domain, we decompose the spectral density matrices containing all the given processes into decomposed spectral matrices

$$\mathbf{G}_f(\omega) = \mathbf{D}_f(\omega)\mathbf{D}_f^*(\omega) \tag{23}$$

Then at each perturbation order, we obtain

$$\mathbf{D}_{y[0]}(\omega) = \mathbf{H}^{[0]}(\omega)\mathbf{D}_f(\omega); \qquad \mathbf{D}_{y[1]}(\omega) = \mathbf{H}^{[1]}(\omega)\mathbf{D}_{x[0]}(\omega) \tag{24a,b}$$

and

$$\mathbf{D}_{y[2]}(\omega) = \mathbf{H}^{[2]}(\omega)\begin{bmatrix}\mathbf{D}_{y[0]}(\omega)\\ \mathbf{D}_{x[1]}(\omega)\end{bmatrix} \tag{24c}$$

The response decomposed spectra is simply a summation of all the decomposed spectra at different perturbation orders

$$\mathbf{D}_x(\omega) = \sum_{r=0}^{\infty} \mathbf{D}_{x[r]}(\omega) \tag{25}$$

which leads to the cross-spectral matrix of the response given by (13). As for the iteration procedure, each iteration is given by

$$\mathbf{D}_{x(r)} = \mathbf{H}^{(r)}(\omega)\mathbf{D}_f(\omega) \tag{26}$$

and the decomposed spectra of the error function is

$$\mathbf{D}_e(\omega) = \mathbf{D}_{x(r)}(\omega) - \mathbf{D}_{x(r-1)}(\omega) \tag{27}$$

which leads to $\mathbf{G}_e(\omega)$ given by (13).

It needs to be emphasized that the stochastic decomposition technique is not an approximation of conventional spectral analysis. No information is lost following the decomposition. Mathematically, these two methods lead to precisely the same solution. The method presented herein is computationally more efficient than conventional spectral analysis as applied to the cascade systems.

SPECTRAL MATRIX DECOMPOSITION

The decomposition of $\mathbf{G}_y(\omega)$ in (13) is not unique, and thus the resulting decomposed spectra are not unique either. Regardless of the decomposition not being unique, the parent spectral matrix is uniquely defined by any decomposed matrices. There are many approaches to realize (13). Typically, we can use the Cholesky decomposition as follows:

$$D_{y_{\mu/\mu}}(\omega) = \left\{G_{y_{\mu\mu}}(\omega) - \sum_{\lambda=1}^{\mu-1} [D_{y_{\mu/\lambda}}(\omega)\overline{D_{y_{\mu/\lambda}}(\omega)}]\right\}^{1/2} \tag{28a}$$

and

$$D_{y_{\nu/\mu}}(\omega) = 0 \qquad \text{if } D_{y_{\mu/\mu}}(\omega) = 0 \tag{28b}$$

otherwise

$$D_{y_{\nu/\mu}}(\omega) = \frac{G_{y_{\mu\nu}}(\omega) - \sum_{\lambda=1}^{\mu-1} D_{y_{\mu/\lambda}}(\omega)\overline{D_{y_{\nu/\lambda}}(\omega)}}{D_{y_{\mu/\mu}}} \tag{28c}$$

with $\mu = 1, 2, \ldots, M$ and $\nu = i + 1, i + 2, \ldots, N$.

Let the dimension of the decomposed spectral matrix be $M \times \Lambda$; Λ is M minus the number of elements of $D_{y_{\mu/\mu}}(\omega) = 0$ in (28*b* and *c*). Λ is named as the decomposition order here and is equal to the rank of the spectral matrix. It is also a function of ω, that is, $\Lambda(\omega)$. A lower decomposition order helps to further reduce the necessary computational effort. The decomposition order can be kept lower by introducing approximations. Consider the μth time process consisting of a number of mutually noncoherent component processes as in (18), the standard deviation of the μth process can be written as

$$\sigma_{y_\mu} = \sqrt{\sum_{\lambda=1}^{\Lambda} \sigma^2_{y_{\mu/\lambda}}} \tag{29}$$

in which σ denotes the standard deviation of a process. Hence, neglecting a component process with less energy has little effect on the total energy of the process. The Cholesky decomposition procedure is helpful in determining the energy level. Let us add an extra condition to (28*a*)

$$D_{y_{\mu/\mu}}(\omega) = 0 \quad \text{if } 1 - \frac{\sum_{\lambda=1}^{\mu-1} D_{y_{\mu/\lambda}}(\omega)\overline{D_{y_{\mu/\lambda}}(\omega)}}{G_{y_{\mu/\mu}}(\omega)} < T_{ol} \tag{30}$$

where T_{ol} = an error tolerance. Accordingly, the decomposition order is reduced.

EXAMPLE—FREQUENCY-DOMAIN MOTION ANALYSIS OF MOORED STRUCTURES

Governing Equations

The dynamic response analysis procedure of a moored floating offshore platform, exposed to random wind and wave fields is used to demonstrate the effectiveness of this approach. Moored platforms, for example, semisubmersibles and tension leg platforms are being used for deepwater oil drilling and production. The deck of a moored platform is supported by the buoyancy force of columns and pontoons. The wind-induced and ocean-wave-induced forces are resisted by the mooring systems, such as flexible mooring lines and tethers. Typically in the global motion analysis, the entire deck structure is viewed as a rigid body with six degree-of-freedom motions. The mooring system is either represented by massless springs or as a secondary system representing dynamics of the mooring system. The governing equation of the platform motion is given by

$$\mathbf{M}\ddot{\mathbf{X}}(t) + (\mathbf{C}_{\text{str}} + \mathbf{C}_{\text{rad}})\dot{\mathbf{X}}(t) + \mathbf{K}\mathbf{X}(t) = \mathbf{F}(t) \tag{31}$$

in which $\mathbf{X}(t)$ represents six degree-of-freedom rigid-body motions; $\mathbf{M}$, $\mathbf{C}_{\text{str}}$, $\mathbf{C}_{\text{rad}}$, and $\mathbf{K}$ = mass (including water-added mass) matrix, structural and radiation damping matrix and stiffness matrix due to mooring systems (6, 6), respectively; and $\mathbf{F}(t)$ represents the wind and wave loads acting on the platform (6 degrees of freedom). All of these vectors are referred to the rigid-body coordinate system ($O\ X_1\ X_2\ X_3$) (Fig. 4). The wind condition is given by the cross-spectral description of the wind velocity field, which is used to obtain the cross-spectral density matrix (6, 6) $\mathbf{G}_A(\omega)$ of wind loads acting on the platform in terms of six degrees of freedom (Kareem and Dalton 1982; Kareem 1985). The wave field is described by the spectrum of wave surface elevation $\eta(t)$ at a reference location. The wave forces can be divided into the potential and drag forces (Sarpkaya and Isaacson 1981). The potential force on the structure can be described by the diffraction theory or the inertia term in the Morison equation, depending on the ratio between the wavelength and platform component sizes. Accordingly, the wave forces of the potential origin in the six degrees of platform motion $\mathbf{F}_{\text{pot}}(t)$ can be expressed as a linear transform of $\eta(t)$. The transfer function $\mathbf{H}_{\text{pot}}(\omega)$ in this case can be derived from a boundary-element diffraction code [e.g., Kareem and Li (1988)].

The drag force is related nonlinearly to the relative fluid-structure velocity. If the immersed parts of the structure are discretized into N_c components, the drag force on the αth component, in terms of three degrees of freedom with respect to each component's fixed frame, is given by

$$\mathbf{f}_{d_\alpha}(t) = C_{d_\alpha}\mathbf{v}_\alpha(t)|\mathbf{v}_\alpha(t)| \tag{32}$$

where C_{d_α} is a local drag coefficient. The relative fluid-structure velocity $\mathbf{v}_\alpha(t)$, is equal to the difference between the water particle velocity vector at the αth component $\mathbf{u}_\alpha(t)$ and the velocity vector of the motion of the αth platform component $\dot{\mathbf{x}}_\alpha(t)$

$$\mathbf{v}_\alpha(t) = \mathbf{u}_\alpha(t) - \dot{\mathbf{x}}_\alpha(t) \tag{33}$$

In the preceding equation, vectors $\mathbf{v}_\alpha(t)$, $\mathbf{u}_\alpha(t)$, and $\dot{\mathbf{x}}_\alpha(t)$ are referred to the local coordinate system ($o_i\ x_{1_i}\ x_{2_i}\ x_{3_i}$) (see Fig. 4 for coordinate system). According to the linear wave theory, $\mathbf{u}_\alpha(t)$ is a linear transform of $\eta(t)$ and the transfer function $\mathbf{H}_{u_\alpha\eta}(\omega)$, for deep water is given below

$$\mathbf{H}_{u_\alpha\eta}(\omega) = \mathbf{T}_\alpha \begin{Bmatrix} \omega \exp(-k\zeta_\alpha + jk\xi_\alpha) \\ j\omega \exp(-k\zeta_\alpha + jk\xi_\alpha) \\ 0 \end{Bmatrix} \tag{34}$$

where $\mathbf{T}_\alpha$ = the transformation matrix (3, 2) from space-fixed coordinates ($o\ \xi\ \zeta$) to local coordinates ($o_\alpha x_{\alpha_1} x_{\alpha_2} x_{\alpha_3}$) (see Fig. 4); ζ_α and ξ_α = locations of the center of the αth component relative to the reference location in the vertical and horizontal directions along the direction of wave propagation, and k and ω are wave number and frequency, respectively. The αth component of platform velocity vector $\dot{\mathbf{x}}_\alpha(t)$ is related to the rigid-body platform through a transformation matrix

$$\dot{\mathbf{x}}_\alpha(t) = \mathbf{T}_\alpha\dot{\mathbf{X}}(t) \tag{35}$$

Accordingly then, the global drag force is given by

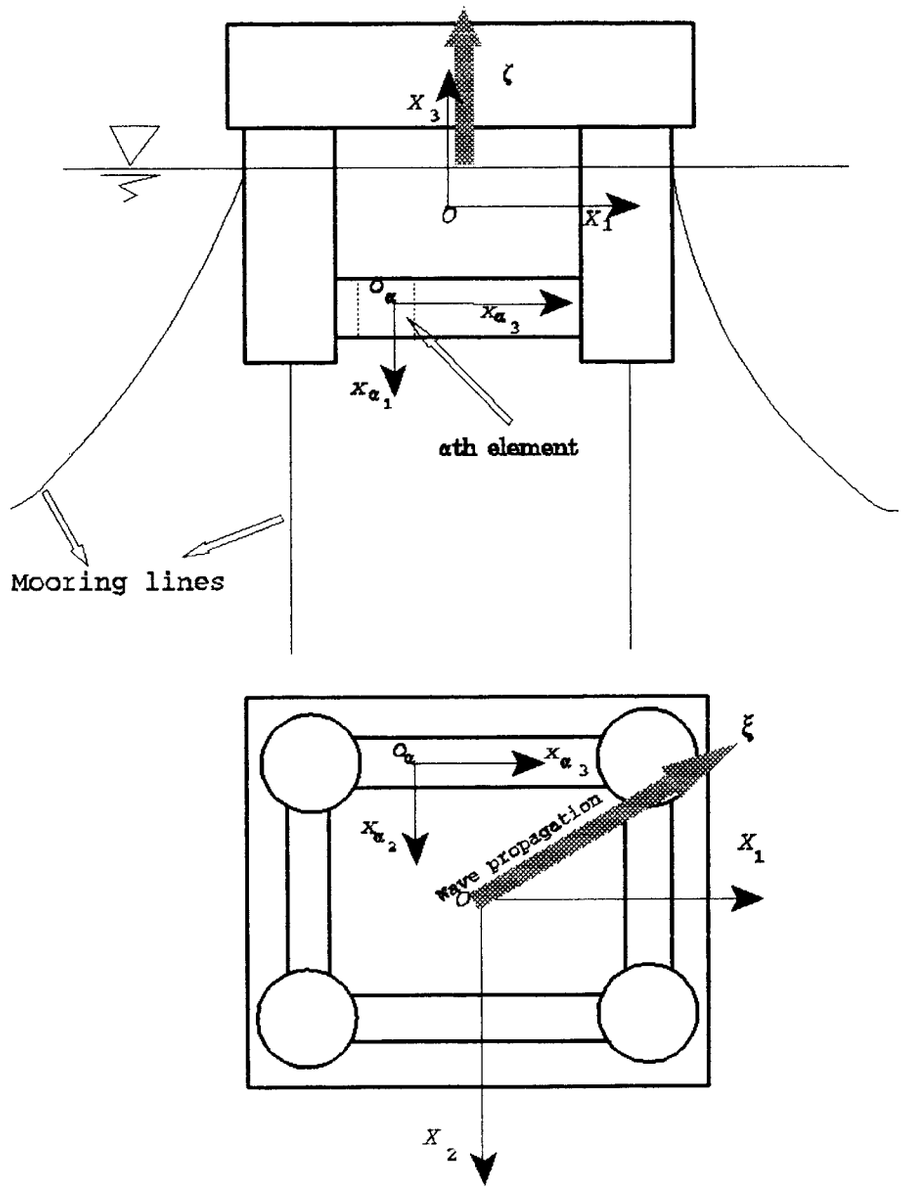

FIG. 4. Coordinate Systems of Floating Platform

$$\mathbf{F}_{\text{drag}}(t) = \sum_{\alpha=1}^{N_c} \mathbf{T}_\alpha^T \mathbf{f}_{d_\alpha}(t) \tag{36}$$

where $\mathbf{f}_{d_\alpha}(t)$ = drag force on the αth component in local coordinates. However, the nonlinear relationship in (32) makes the frequency domain analysis difficult. Some mathematical manipulations involving linearization lead to the following approximate equation [e.g., Eatock-Taylor and Rajagopalan (1982); Li and Kareem (1993)]

$$\mathbf{f}_{d_\alpha}(t) \approx \mathbf{Q}_\alpha(\text{Cov}_\alpha)\mathbf{v}_\alpha(t) \tag{37}$$

where $\mathbf{Q}_\alpha(\text{Cov}_\alpha)$ is a coefficient matrix (3, 3) and it is a function of the covariance matrix of $\mathbf{v}_\alpha(t)$. Hence, (31) can be rearranged as

$$\mathbf{M}\ddot{\mathbf{X}}(t) + \mathbf{C}(\text{Cov})\dot{\mathbf{X}}(t) + \mathbf{K}\mathbf{X}(t) = \hat{\mathbf{F}}(t) \tag{38}$$

where the damping coefficient matrix is a summation of the structural, radiation, and drag damping. The drag-damping term is a function of the covariance of the fluid-structure relative velocities. Total damping is given by

$$\mathbf{C}(\text{Cov}) = \mathbf{C}_{\text{str}} + \mathbf{C}_{\text{rad}} + \sum_{\alpha=1}^{N_c} \mathbf{T}_\alpha^T \mathbf{Q}_\alpha(\text{Cov}_\alpha)\mathbf{T}_\alpha \tag{39}$$

and the load vector in the right-hand side is

$$\hat{\mathbf{F}}(t) = \mathbf{F}_{\text{pot}}(t) + \hat{\mathbf{F}}_{\text{drag}}(t) + \mathbf{F}_{A}(t) \tag{40}$$

In the preceding equation, the exciting-wave drag-force vector $\hat{\mathbf{F}}_{\text{drag}}(t)$ is a function of the covariance of the fluid-structure relative velocities

$$\hat{\mathbf{F}}_{\text{drag}}(t) = \sum_{\alpha=1}^{N_c} \mathbf{T}_{\alpha}^{T}\mathbf{Q}_{\alpha}(\text{Cov}_{\alpha})\mathbf{H}_{u_{\alpha}\eta}\eta(t) \tag{41}$$

Conventional Spectral Analysis Procedure

Before proceeding to the analysis based on the stochastic decomposition, conventional spectral analysis is briefly introduced. Following (34–36), and so on, the global spectral matrix (6, 6) of wave forces, $\hat{\mathbf{F}}_{w}^{(r)}(t)$, that include both the potential and drag forces, in the rth iteration is given by

$$\mathbf{G}_{\hat{F}_w}^{(r)}(\omega) = \left(\mathbf{H}_{\text{pot}}(\omega) + \sum_{\alpha=1}^{N_c} \mathbf{T}_{\alpha}^{T}\mathbf{Q}_{\alpha}(\text{Cov}_{\alpha}^{(r-1)})\mathbf{H}_{u_{\alpha}\eta}(\omega)\right) G_{\eta}(\omega) \cdot \left(\mathbf{H}_{\text{pot}}(\omega) + \sum_{\alpha=1}^{N_c} \mathbf{T}_{\alpha}^{T}Q_{\alpha}(\text{Cov}_{\alpha}^{(r-1)})\mathbf{H}_{u_{\alpha}\eta}(\omega)\right)^{*} \tag{42}$$

where the coefficient $\mathbf{Q}_{\alpha}(\text{Cov}_{\alpha}^{(r-1)})$, defined previously in (37), is obtained from the preceding iteration. By assuming that the wind and wave forces are uncorrelated, the total environmental loading on a platform is given by

$$\mathbf{G}_{\hat{F}}^{(r)}(\omega) = \mathbf{G}_{\hat{F}_w}^{(r)} + \mathbf{G}_{F_A}(\omega) \tag{43}$$

The global response spectral matrix can be obtained by

$$\mathbf{G}_{X}^{(r)}(\omega) = \mathbf{H}^{(r)}(\omega)\mathbf{G}_{F}^{(r)}(\omega)\mathbf{H}^{(r)*}(\omega) \tag{44}$$

in which the system transfer function is based on the equation of motion given in (38)

$$\mathbf{H}^{(r)}(\omega) = (-\omega^2\mathbf{M} - j\omega\mathbf{C}(\text{Cov})^{(r-1)} + \mathbf{K})^{-1} \tag{45}$$

For the next iteration, the spectral matrix of the relative fluid-structure velocities needs to be computed to evaluate $\mathbf{C}(\sigma)$ in the transfer function. This spectral matrix is given by

$$\mathbf{G}_{v_{\alpha}}^{(r)}(\omega) = \mathbf{G}_{u_{\alpha}}(\omega) + \mathbf{G}_{\dot{x}_{\alpha}}^{(r)}(\omega) - \mathbf{G}_{u_{\alpha}\dot{x}_{\alpha}}^{(r)}(\omega) - \mathbf{G}_{u_{\alpha}\dot{x}_{\alpha}}^{(r)*}(\omega) \tag{46}$$

in which the first two spectral density functions can be obtained in a straightforward manner

$$\mathbf{G}_{\dot{x}_{\alpha}}^{(r)}(\omega) = (\mathbf{T}_{\alpha}^{(r)}j\omega)\mathbf{G}_{X}^{(r)}(\omega)(\mathbf{T}_{\alpha}^{(r)}j\omega)^{*} \tag{47}$$

and

$$\mathbf{G}_{u_{\alpha}}(\omega) = \mathbf{H}_{u_{\alpha}\eta}(\omega)G_{\eta}\mathbf{H}_{u_{\alpha}\eta}^{*}(\omega) \tag{48}$$

The third term, $G_{u_{\alpha}\dot{x}_{\alpha}}^{(r)}(\omega)$ (3, 3), however, involves a series of matrix operations. As alluded to earlier, these computations can become quite extensive for platforms that are discretized into a large number of elements.

Frequency Domain Procedure by Stochastic Decomposition Method

The stochastic decomposition approach precludes computation of the cross-spectral matrices. The computational procedure is illustrated in Table 1 and detailed in the following section.

The decomposed spectral density function, $D_{\eta}(\omega)$, for the wave surface elevation and the decomposed spectral matrix, $\mathbf{D}_{F_A}(\omega)$ (6, 6), for the wind loads are given below

$$D_{\eta}(\omega)D_{\eta}(\omega) = \sqrt{G_{\eta}(\omega)} \tag{49}$$

and

$$\mathbf{D}_{F_A}(\omega)\mathbf{D}_{F_A}^{*}(\omega) = \mathbf{G}_{F_A}(\omega) \tag{50}$$

The associated potential wave forces and the water velocities are represented by their respective decomposed spectra, $\mathbf{D}_{F_{\text{pot}}}(\omega)$ (6, 1) and $\mathbf{D}_{u_i}(\omega)$ (3, 1) as

$$\mathbf{D}_{F_{\text{pot}}}(\omega) = \mathbf{H}_{\text{pot}}(\omega)D_{\eta}(\omega) \tag{51a}$$

and

TABLE 1. Response Computation of Compliant Platform by Stochastic Decomposition

Process item (1)	Wave related $\mu = 0$ (2)	Wind Related $\mu =$ 1 (3)	2, 3, 4, 5 (4)	6 (5)	Equation (6)
Wind force (6×1) $\mathbf{F}_a(t)$	—	$\mathbf{F}_{A_1}(t)$	$\cdots$	$\mathbf{F}_{A_6}(t)$	(50)
Wave surface elevation	$\eta(t)$	—	—	—	(49)
Wave potential force (6×1)	$\mathbf{F}_{\text{pot}}(t)$	—	—	—	(51*a*)
Wave practical velocities (3×1) $\alpha = 1, 2, \ldots, N_c$	$\mathbf{u}_\alpha(t)$	—	—	—	(51*b*)
Wave drag force (6×1)	$\hat{\mathbf{F}}^{(r)}_{\text{drag}}(t)$	—	—	—	(53)
Applied loads (6×1) $\hat{\mathbf{F}}^{(r)}(t)$	$\mathbf{F}_{\text{pot}}(t) + \hat{\mathbf{F}}^{(r)}_{\text{drag}}(t)$	$\mathbf{F}_{A_1}(t)$	$\cdots$	$\mathbf{F}_{A_6}(t)$	(54)
Displacement response (6×1) $\mathbf{X}^{(r)}(t)$	$\mathbf{X}^{(r)}_0(t)$	$\mathbf{X}^{(r)}_1(t)$	$\cdots$	$\mathbf{X}^{(r)}_6(t)$	(55)
Velocity response (6×1) $\dot{\mathbf{X}}^{(r)}(t)$	$\dot{\mathbf{X}}^{(r)}_0(t)$	$\dot{\mathbf{X}}^{(r)}_1(t)$	$\cdots$	$\dot{\mathbf{X}}^{(r)}_6(t)$	(59)
Local velocities (3×1) $\dot{\mathbf{x}}^{(r)}_\alpha(t)$	$\dot{\mathbf{x}}^{(r)}_{\alpha/0}(t)$	$\dot{\mathbf{x}}^{(r)}_{\alpha/1}(t)$	$\cdots$	$\dot{\mathbf{x}}^{(r)}_{\alpha/6}(t)$	(60)
Relative velocities (3×1) $\mathbf{v}^{(r)}_\alpha(t)$	$\mathbf{u}_\alpha(t) - \dot{\mathbf{x}}^{(r)}_{\alpha/0}(t)$	$-\dot{\mathbf{x}}^{(r)}_{\alpha/1}(t)$	$\cdots$	$-\dot{\mathbf{x}}^{(r)}_{\alpha/6}(t)$	(61)
Convergence $e^{(r)}(t)$	$e^{(r)}_0(t)$	$e^{(r)}_1(t)$	$\cdots$	$e^{(r)}_6(t)$	(56)

$$\mathbf{D}_{u_\alpha}(\omega) = \mathbf{H}_{u_\alpha}(\omega) D_\eta(\omega) \tag{51b}$$

Accordingly, the wind load is decomposed into six noncoherent vector subprocesses

$$\mathbf{F}_A(t) = \sum_{\lambda=1}^{6} \mathbf{F}_{A_\lambda}(t) \tag{52}$$

At the rth iteration, the exciting drag force is given by

$$\mathbf{D}^{(r)}_{F_{\text{drag}}}(\omega) = \sum_{\alpha=1}^{N_c} \mathbf{T}^T_\alpha \mathbf{Q}_\alpha (\text{Cov}^{(r-1)}_\alpha) \mathbf{D}_{u_\alpha}(\omega) \tag{53}$$

By taking into consideration that the potential and wave drag forces are fully coherent and that they are noncoherent with the wind force, we can write the total applied load $\mathbf{F}^{(r)}(t)$ in terms of seven mutually noncoherent subprocess $\mathbf{F}_{\mu/\lambda}(t)$ among which $\mathbf{F}_{\mu/}(t) = (\mathbf{F}_{A_\mu}(t)$ for $\mu = 1$–6, and $\mathbf{F}^{(r)}_{0/}(t) = \mathbf{F}_{\text{pot}}(t) + \hat{\mathbf{F}}^{(r)}_{\text{vis}}(t)$. The corresponding decomposed spectral matrix, $\mathbf{D}^{(r)}_F(\omega)$, is expressed as

$$\mathbf{D}^{(r)}_F(\omega) = [\mathbf{D}_{F_A}(\omega)(\mathbf{D}_{\text{pot}}(\omega) + \mathbf{D}^{(r)}_{F_{\text{vis}}}(\omega))] \tag{54}$$

The decomposed spectral matrix function (6, 7) of global response at the rth iteration is

$$\mathbf{D}^{(r)}_X(\omega) = \mathbf{H}^{(r)}(\omega) \mathbf{D}^{(r)}_F(\omega) \tag{55}$$

The convergence is checked by the decomposed spectral error matrices (6, 6)

$$\mathbf{D}_e(\omega) = \mathbf{D}^{(r)}_X(\omega) - \mathbf{D}^{(r-1)}_X(\omega) \tag{56}$$

If all the elements of the matrix

$$\text{Cov}_e = \int_0^\infty \mathbf{D}_e(\omega) \mathbf{D}^*_e(\omega)\, d\omega \tag{57}$$

are less than a prescribed value, the computation is completed. The cross-spectral density matrix of the response is simply given by

$$\mathbf{G}_X(\omega) = \mathbf{D}^{(r)}_X(\omega) \mathbf{D}^{(r)*}_X(\omega) \tag{58}$$

However, if the convergence criterion is not satisfied, the iteration process must be continued and the input to the next iteration is prepared. The global velocities are first expressed as

$$\mathbf{D}^{(r)}_{\dot{X}}(\omega) = -j\omega \mathbf{D}^{(r)}_X(\omega) \tag{59}$$

The local velocities (3, 7 matrix function) are given by

$$\mathbf{D}^{(r)}_{\dot{x}_\alpha}(\omega) = \mathbf{T}_\alpha \mathbf{D}^{(r)}_{\dot{X}}(\omega) \tag{60}$$

The relative velocities [in (33)], related with waves and winds, are respectively represented by

$$\mathbf{D}^{(r)}_{v_{\alpha/0}}(\omega) = \mathbf{D}_{u_\alpha}(\omega) - \mathbf{D}^{(r)}_{\dot{x}_{\alpha/0}}(\omega) \tag{61a}$$

and

$$\mathbf{D}^{(r)}_{v_{\alpha/\mu}}(\omega) = -\mathbf{D}^{(r)}_{\dot{x}_{\alpha/\mu}}(\omega); \qquad \text{for } \mu = 1, 2, \ldots, 6 \tag{61b}$$

An integration of the decomposed spectra of the relative velocities leads to the covariances of the relative velocities

$$\text{Cov}_{\alpha}^{(r)} = \int_0^{\infty} \mathbf{D}_{\dot{r}_\alpha}^{(r)}(\omega)\mathbf{D}_{\dot{r}_\alpha}^{(r)*}(\omega)\, d\omega \tag{62}$$

This is then used to obtain the new transfer function for the next iteration.

In the procedure shown, by using the stochastic decomposition technique, each transformation only involves matrix multiplication with dimension less than seven. The cross-spectral density-function calculation is totally eliminated. Computational effort in terms of matrix multiplication is only one-third of that required for conventional spectral analysis. If the convergence criterion described by (10) is introduced, the difference is much larger. Table 1 presents the relationship among all decomposed subprocesses, including the given, intermediate, and final solution, and offers a flowchart of the analysis procedure. The last column in this table indicates equation numbers corresponding to each variable that provides a convenient reference for tracking the computational procedure. In Table 1, all the component processes in the same column are fully coherent, and any two component processes in different columns are noncoherent.

Further applications of this approach in offshore mechanics include response of a moored floating system in multicorrelated wind and multidirectional seas. The response due to second-order effects, for example, low-frequency drift can be conveniently obtained by using the stochastic decomposition concept for quadratic systems. Details will be addressed in a future publication.

CONCLUDING REMARKS

A stochastic decomposition technique is presented that helps to improve the efficiency of the frequency-domain analysis of a nested-cascade dynamic system by eliminating the need for estimating the cross-spectral density matrix involving the input, intermediate, and output vectors. The perturbation-based and iteration-based frequency-domain analyses can be conveniently represented by nested-cascade systems, thus permitting use of the stochastic decomposition approach to the frequency-domain analysis. Central to this technique is the decomposition of a set of correlated random processes into a number of component random subprocesses. Statistically, any two decomposed processes are either fully coherent or noncoherent. Each random subprocess is characterized by a decomposed spectrum that is related to conventional spectral descriptions, for example, spectral density function or a cross-spectral density function. Any linear transformation that relates a set of random processes also describes the corresponding decomposed spectral descriptions of these processes. Mathematically, the conventional spectral transformation and the transformation of decomposed spectra lead to the same final results, but the latter is computationally more efficient. The effectiveness of this methodology is demonstrated by means of an example concerning the stochastic response of a moored offshore platform exposed to wind and wave loads. Clearly, the application of stochastic decomposition facilitates a convenient analysis of the response at only a fraction of the time needed to carry out the conventional spectral analysis.

ACKNOWLEDGMENTS

The support of this research was provided in part by the National Science Foundation Grant No. ECE-8352223 (BCS-90-96374), ONR Grant No. N00014-93-1-0761, and several industrial sponsors.

APPENDIX. REFERENCES

Bendat, J. S. (1977). "Procedure for frequency decomposition of multiple input/output relationships." *Stochastic problems in dynamics*, B. L. Clarkson, ed., Pitman, London, England, 308–322.

Deleuil, G. E., Des Deserts, L. D., Doris, C. G., and Shive, A. (1986). "A new method for frequency domain analysis of offshore structure: comparison with time domain analysis." *OTC 5303, Proc., Offshore Technology Conference*, Richardson, Tex.

Dodds, C. J., and Robson, J. D. (1975). "Partial coherence in multivariate random processes." *J. Sound and Vibration*, 42(2), 243–249.

Eatock, T. R., and Rajagopalan, A. (1982). "Dynamics of offshore structure, part I: perturbation analysis." *J. Sound and Vibration*, 83(3), 401–416.

Grecco, M. G., and Hudspeth, R. T. (1983). "Stochastic response of prototype offshore structure." *J. Struct. Engrg.*, ASCE, 109(5), 1119–1138.

Kareem, A., and Li, Y. (1988). "Stochastic response of a tension leg platform to wind and wave loads." *Tech. Rep. No. UHCE88-18*, Department of Civil Engineering, University of Houston, Houston, Tex.

Kareem, A. (1985). "Wind-induced response analysis of tension leg platforms." *J. Struct. Engrg.*, ASCE, 111(1), 37–55.

Kareem, A., and Dalton, C. (1982). "Dynamic effects of wind on tension leg platforms." *OTC 4229, Proc., Offshore Technology Conference*, Richardson, Tex.

Li, Y., and Kareem, A. (1993). "Multivariate hermite expansion of hydrodynamic drag loads on tension leg platforms." *J. Engrg. Mech.*, ASCE, 119, 91–112.

Lipsett, A. W. (1986). "Nonlinear structural response to random waves." *J. Struct. Engrg.*, ASCE, 112(11), 2416–2429.
Sarpkaya, T., and Isaacson, M. (1981). *Mechanics of wave forces on offshore structure*. Van Nostrand Reinhold, New York, N.Y.
Shinozuka, M. (1963). "Simulation of multivariate and multidimensional random processes." *J. Acoustic Soc. of Am.*, 4, 29–36.